Side-Chain Effect on Cyclopentadithiophene/Fluorobenzothiadiazole-Based Low Band Gap Polymers and Their Applications for Polymer Solar Cells

ARTICLE *in* MACROMOLECULES · JUNE 2013

Impact Factor: 5.8 · DOI: 10.1021/ma4009302

11 AUTHORS, INCLUDING:

Hin-Lap Yip
South China University of Technology
123 PUBLICATIONS **6,894** CITATIONS
SEE PROFILE

Chu-Chen Chueh
University of Washington Seattle
63 PUBLICATIONS **1,851** CITATIONS
SEE PROFILE

Jeremy J Intemann
University of Washington Seattle
19 PUBLICATIONS **276** CITATIONS
SEE PROFILE

Alex K-Y Jen
University of Washington Seattle
391 PUBLICATIONS **15,968** CITATIONS
SEE PROFILE

Macromolecules

Article

pubs.acs.org/Macromolecules

Side-Chain Effect on Cyclopentadithiophene/Fluorobenzothiadiazole-Based Low Band Gap Polymers and Their Applications for Polymer Solar Cells

Yongxi Li,[†,‡] Jingyu Zou,[†] Hin-Lap Yip,[†] Chang-Zhi Li,[†] Yong Zhang,[†] Chu-Chen Chueh,[†] Jeremy Intemann,[†] Yunxiang Xu,[†] Po-Wei Liang,[†] Yu Chen,[‡,*] and Alex K.-Y. Jen[†,*]

[†]Department of Materials Science and Engineering, University of Washington, Seattle, Washington 98195, United States

[‡]Key Lab for Advanced Materials, Institute of Applied Chemistry, East China University of Science and Technology, 130 Mei Long Road, Shanghai 200237, China

Supporting Information

ABSTRACT: A series of cyclopentadithiophene-based low band gap conjugated polymers with varied side-chain patterns and F-substituents were synthesized. By replacing the shorter 2-ethylhexyl (EH) side-chain with the longer 3,7-dimethyloctyl (DMO) side-chain, it resulted in significant changes to the optical, electrochemical, and morphological properties of the polymers, as well as the subsequent performance of devices made from these materials. Solar cells fabricated from polymer with 2-ethylhexyl (EH) side-chain and monofluoro substituent exhibits increased open circuit voltage, short circuit current and fill factor, resulting in the highest power conversion efficiency (5.5%) in this series of polymers. This finding provides valuable insight for making more efficient low band gap polymers.

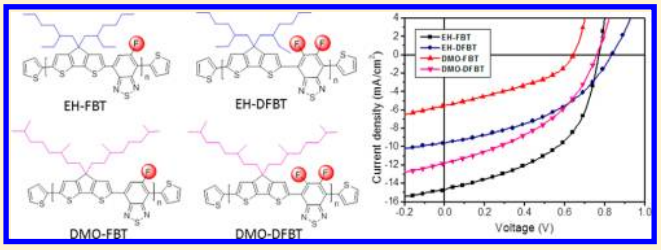

Recent progress on developing p-type conjugated polymers has led to significant advances in polymer solar cells (PSCs). Power conversion efficiency (PCE) of single junction PSCs have already exceeded 9% in several recently reported devices.[1] However, there are still challenges that need to be addressed in order to further improve the performance of these devices.[2−6] The main limitations lie on that the polymers used cannot absorb light efficiently to generate enough charge carriers and their intrinsically low charge mobility. By stacking both large and small band gap polymers into a tandem solar cell, it can enhance light absorption and PCE.

However, one of the problems that strongly impedes the progress of tandem solar cell development is the lacking of high-performance low band gap polymers (E_g < 1.5 eV).[7−18] Therefore, it is important to develop suitable small band gap polymers that can be used to fabricate PSCs with reduced energy loss and increased photocurrent density.

Recently, poly[2,6-(4,4-bis(2-ethylhexyl)-4*H*-cyclopenta[2,1-*b*;3,4-*b*′]dithiophene)-*alt*-4,7-(monofluoro-2,1,3-benzothiadiazole)] (PCPDTFBT) has been reported by both Jen[19] and Neher[20] as an efficient small band gap (1.44 eV) polymer. A relatively high PCE of 5.51% could be obtained without using additional solvent additives during device fabrication. The resulting devices could reach an open-circuit voltage (V_{oc}) of 0.75 V and a short-circuit current density (J_{sc}) of 15.0 mA cm^{-2}. However, these devices only showed a relatively low fill factor (FF) of 0.49. Although this polymer can be considered for use in tandem solar cells, its high lying highest occupied molecular orbital (HOMO) energy level limits the V_{oc} of the resultant cell.

Owing to the electron-withdrawing character of fluorine (F) atom, conjugated polymers with F groups functionalized on their backbones usually exhibit lower HOMO energy levels, thus it can increase the V_{oc} of the corresponding device.[21−26] We have previously introduced difluorobenzothiadiazole to further deepen the HOMO level of the PCPDTFBT polymer. As expected, the new polymer poly[2,6-(4,4-bis(2-ethylhexyl)-4*H*-cyclopenta[2,1-*b*;3,4-*b*′]dithiophene)-*alt*-4,7-(difluoro-2,1,3-benzothiadiazole)] (PCPDTDFBT) showed an increased V_{oc} of 0.84 eV, which is about ∼0.1 eV higher than that of PCPDTFBT. This V_{oc} is one of the highest among currently available low band gap polymers. Nonetheless, the solubility of PCPDTDFB is quite poor due to enhanced F−H, F−F interactions and strong stacking of polymer. It strongly limits its processability, which can only be processed through hot o-DCB. This not only hampers the formation of good quality film, but also creates significant problem for device fabrication.

In order to generate high V_{oc} while maintaining good solution processability of the polymer, we have devoted significant efforts in engineering its alkyl side-chains. This has been proven to be an effective way to modulate the solubility of polymers. Recently, Müllen[22] has demonstrated that longer linear alkyl chains C_{16} could be used to replace shorter branched $C_{2,8}$ to enhance packing of polymer chains to achieve very high mobility (3.3 cm^2 V^{-1} s^{-1}). Pei[27] has also reported

Received: May 3, 2013
Revised: June 21, 2013
Published: June 28, 2013

Scheme 1. Chemical Structure of Polymers EH−FBT, EH−DFBT, DMO−FBT, DMO−DFBT

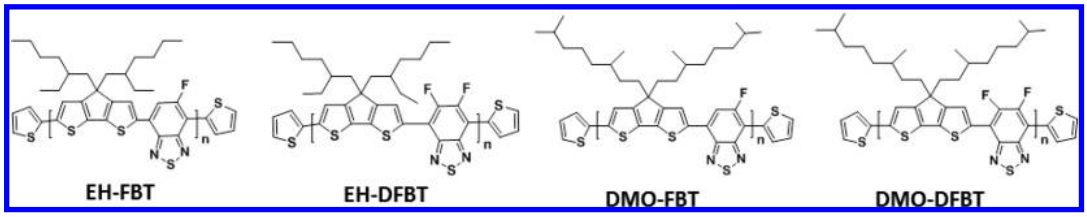

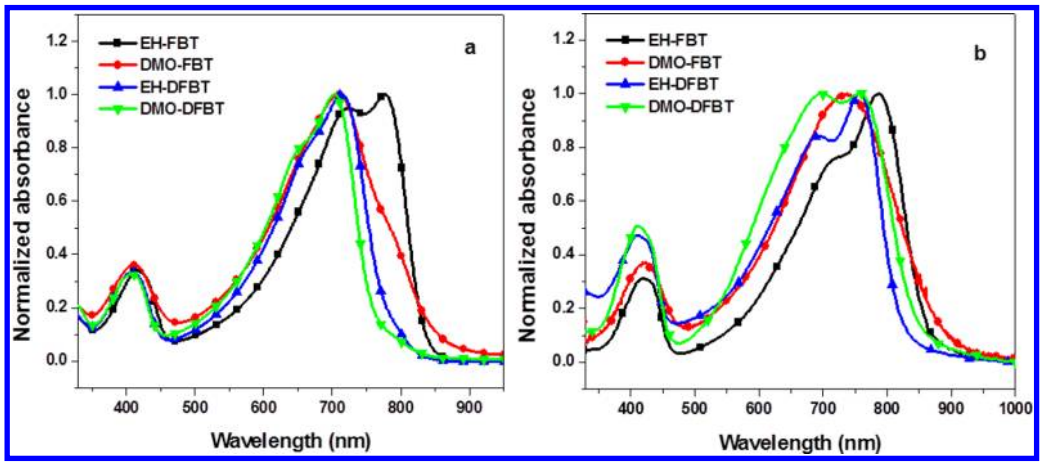

Figure 1. UV−vis spectra of EH−FBT, EH−DFBT, DMO−FBT, and DMO−DFBT in solution (a) and in thin film (b).

significantly enhanced mobility could be achieved through subtle modification of the alkyl chains of isoindigo-based polymers. Very recently, You[28] has also shown significantly improved PCE (form 1.9% to 5.6%) in a series of naphtho[2,1-*b*:3,4-*b*′]dithiophene (NDT) and 4,7-di(thiophen-2-yl)-benzothiadiazole (DTBT) containing conjugated polymers with different side-chains and F-substituents.

Herein, we report the systematic study of a series of cyclopentadithiophene-based conjugated polymers with varied side-chain patterns and F-substitutions for high efficiency low band gap polymers. To our surprise, the replacement of shorter and bulkier 2-ethylhexyl (EH) side-chain with longer 3,7-dimethyloctyl (DMO) side-chain has resulted in significant changes of the optical, electrochemical, and morphological properties of the polymers, as well as the subsequent performance of PSCs made from these materials. To investigate the underlying mechanism for these changes, we have conducted a thorough device, spectroscopic, and theoretical analysis to correlate the structure−performance of these polymers. It was found that the variation of type and length of the alkyl side-chain is critical to the molecular packing behavior. As a result, it caused significant deviation in the photovoltaic properties of polymer devices. This finding may provide insight for making more efficient low band gap polymers.

The chemical structures of four polymers EH−FBT, EH−DFBT, DMO−FBT, DMO−DFBT are shown in Scheme 1 and their synthetic routes are described in Scheme S1, Supporting Information. All reagents were purchased from commercial sources without further purification. The synthetic route of monofluorobenzothiadiazole (FBT) and difluorobenzothiadiazole (DFBT) involves a multistep synthesis starting from 2,5-dibromo-3-fluorobenzene and 2,5-dibromo-3,4-difluorobenzene as shown in our previous work.[24]

Low band gap polymers were synthesized by reacting the corresponding bis(stannyl) compounds (**8a** and **8b**) with monofluorobenzothiadiazole (FBT) and difluorobenzothiadiazole (DFBT) via Stille coupling polymerization. Because of poor solubility of these polymers, it is difficult to achieve high molecular weight by conventional condition. We employed the microwave-assisted Stille polymerization, which was previously demonstrated to be able to increase the molecular weight of resulting polymers.[29] The resulting polymers were collected by precipitating the polymer solution in methanol and filtered. They were washed in a Soxhlet extractor sequentially with acetone, hexane, and chloroform to remove oligomers and residual catalyst. The molecular weight of these polymers were measured by gel permeation chromatography (GPC) using monodispersed polystyrene as the standard and THF as the eluent. These polymers have the number-average molecular weight (M_n) of 25.3, 13.6, 24.6, and 11.2 kg/mol for EH−FBT, EH−DFBT, DMO−FBT, DMO−DFBT, respectively, with a polydispersity index (PDI) of 1.58, 1.56, 1.47, and 1.15. EH−FBT and DMO−FBT are quite soluble in *o*-dichlorobenzene (DCB), chlorobenzene (CB), and *o*-xylene; however, EH−DFBT and DMO−DFBT possess limited solubility because difluorobenzothiadiazole- (DFBT-) based polymers have stronger packing than that of monofluorobenzothiadiazole- (FBT-) based polymers.

UV−vis absorption spectra of cyclopentadithiophene (CPDT) based polymers were investigated in both mixed CB/DCB solutions and in thin film (Figure 1). The data are summarized in Table 1. Because of poor solubility of EH−DFBT, it can only be dissolved in hot *o*-DCB. The rest of the polymers can be dissolved in CB. All these polymers showed two characteristic peaks due to similar polymer main chains (Figure 1a). The longer wavelength band is due to intramolecular charge transfer (ICT) between CPDT and BT units. The twin peaks at the low energy absorption band of EH−FBT

dx.doi.org/10.1021/ma4009302 | *Macromolecules* 2013, 46, 5497−5503

Table 1. Optical and Electrochemical Properties of Polymers

	UV−vis absorption						
	solution		film		cyclic voltammetry		
polymer	λ_{max}/nm	λ_{onset}/nm	λ_{max}/nm	λ_{onset}/nm	HOMO/eV	LUMO/eV	band-gap
EH−FBT	778	830	788	863	−5.03	−3.54	1.49
EH−DFBT	712	780	761	904	−5.16	−3.57	1.59
DMO-FBT	712	864	744	832	−4.96	−3.55	1.41
DMO−DFBT	711	766	761	848	−5.02	−3.57	1.45

(776 nm) are attributed to aggregation resulting from strong polymer chain packing.[23] The thin film absorption spectra of these polymers red-shifted remarkably compared to those measured in solution, which correlated well with polymer packing in solid-state. The new peaks at 757 and 759 nm for EH−DFBT and DMO−DFBT, respectively indicate they may have more ordered structure in the solid-state. Optical band gap of these polymers can be estimated by extrapolating from the absorption edge of these films to be 1.44, 1.37, 1.49, and 1.46 eV for EH−FBT, DMO−FBT, EH−DFBT, and DMO−DFBT, respectively. Interestingly, the absorption spectra of EH−DFBT and DMO−DFBT blue-shifted in both solution and in solid-state compared with those of EH−FBT and DMO−FBT. This may be due to the fluorine atoms have stronger influence on the HOMO of the polymers than on their LUMO, which increase their band gap when difluoro-benzothiadiazole was introduced onto the polymer.

The electrochemical properties of all polymers were investigated by cyclic voltammetry. As shown in Figure 2, the

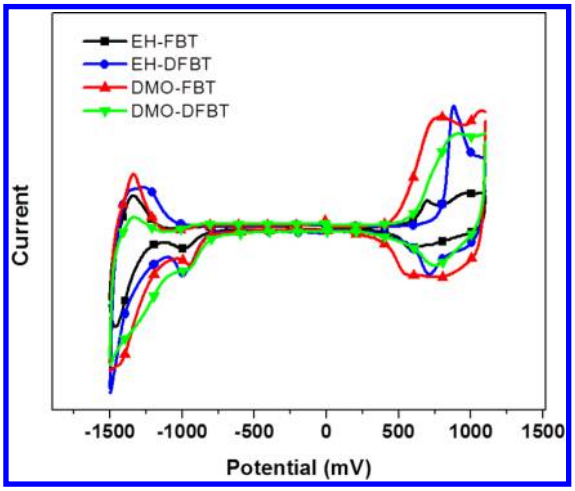

Figure 2. The CV curves of polymers EH−FBT, EH−DFBT, DMO−FBT, and DMO−DFBT films.

redox potentials were measured against Ag/Ag^+ as the reference electrode with a platinum counter electrode in a 0.1 M electrolyte containing tetrabutylammonium hexa fluoro-phosphate in acetonitrile with a scan rate of 100 mV/s. The HOMO/LUMO values of EH−FBT, EH−DFBT, DMO−FBT, and DMO−DFBT were calculated by the onset of the redox potentials taking the known reference level for ferrocene, 4.8 eV below the vacuum level, according to the following equation:[30]

$$\text{HOMO} = -[E_{onset} - E_{ox}(\text{ferrocene})] - 4.8 \text{ eV}$$

$$\text{LOMO} = -[E_{onset} - E_{red}(\text{ferrocene})] - 4.8 \text{ eV}$$

The calculated HOMO values for EH−FBT, EH−DFBT, DMO−FBT,and DMO−DFBT were −5.03, −5.16, −4.96, and −5.02 eV, respectively. The HOMO of EH−DFBT is 0.13 eV deeper than that of EH−FBT after introducing an additional F onto the FBT unit. It is worth to note that the onset of oxidation for EH−FBT and EH−DFBT increased ∼100 mV compared to those of DMO−FBT and DMO−DFBT, despite possessing the same conjugated backbone. This may be due to the decreased Coulombic interactions between the polycationic chains and the anions as the alkyl spacer becomes larger.[31]

To gain deeper insight of the molecular stacking of the polymers, X-ray diffraction analysis of the polymer thin films was performed (Figure 3). The 2θ at 4.5 and 8.0° were related

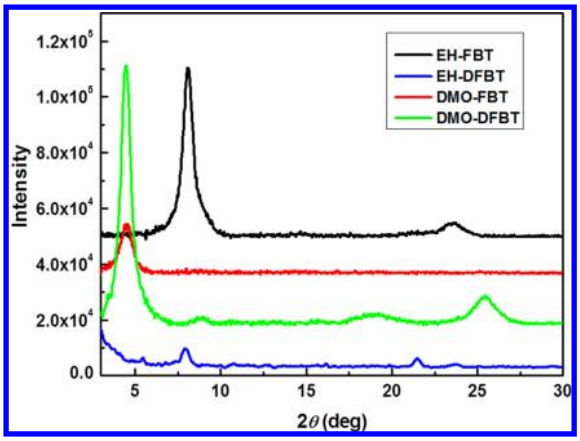

Figure 3. X-ray diffraction analysis of EH−FBT, EH−DFBT, DMO−FBT, and DMO−DFBT after annealing them at 150 °C for 20 min.

to the polymer lamellar spacing, and the stacking distances between coplanar conjugated polymers were represented at 21.5−25.4°. A shorter lamellar spacing of ∼8 Å for the EH-based polymers can be found compare to 19 Å for the DMO based polymer. This can be attributed to the longer side chain length of DMO increasing the spacing. Interestingly, all polymers showed two diffraction peaks except DMO−FBT indicating less structural organization in DMO−FBT film. It was most likely due to the longer and branched DMO side-chains weakening the intermolecular interactions between polymer chains. This hypothesis is supported by the observation from the UV spectra, where EH−FBT, EH−DFBT and DMO−DFBT all showed a shoulder peak at the long wavelengths (resulting from stacking). However, when FBT was replaced with DFBT in DMO−DFBT, a significant change in polymer packing is observed. The polymers showed clear $\pi-\pi$ stacking, which can be attributed to the increased inter- or intramolecular interactions from F−H, F−F interactions. The $\pi-\pi$ stacking distance of DMO−DFBT is shorter (3.5 Å) compared with 3.8 and 4.1 Å, respectively for EH−FBT and EH−DFBT. All these chain spacing are relatively small for semiconducting polymers, which also explains the reason why high mobility could be obtained for OFETs made from these polymers (Table 2).

As the active material for polymer solar cells, high charge carrier mobility is very critical for good device performance since it is directly related to their electronic processes. To probe

dx.doi.org/10.1021/ma4009302 | Macromolecules 2013, 46, 5497−5503

Table 2. OFET Device Performances and XRD Results of Polymers

polymer	d (Å)[a] for L	π	hole mobility ($cm^2\ V^{-1}\ s^{-1}$)	on/off ratio	V_t[b] (V)	electron mobility ($cm^2\ V^{-1}\ s^{-1}$)	on/off ratio	V_t[b] (V)
EH−FBT	11.0	3.8	1.4×10^{-2}	1.0×10^2	−5	1.4×10^{-2}	1.0×10^2	0
EH−DFBT	11.3	4.1	5.0×10^{-4}	1.0×10^2	−22	2.0×10^{-3}	1.0×10^2	21
DMO-FBT	19.6	_	3.0×10^{-4}	6.5×10^3	−22	1.8×10^{-4}	2.0×10^3	36
DMO−DFBT	19.8	3.5	3.5×10^{-4}	6.2×10^3	−21	2.8×10^{-4}	3.9×10^3	34

[a]Lamellar (L) and π−π stacking (π) distances determined by XRD experiments. [b]V_t for threshold voltage.

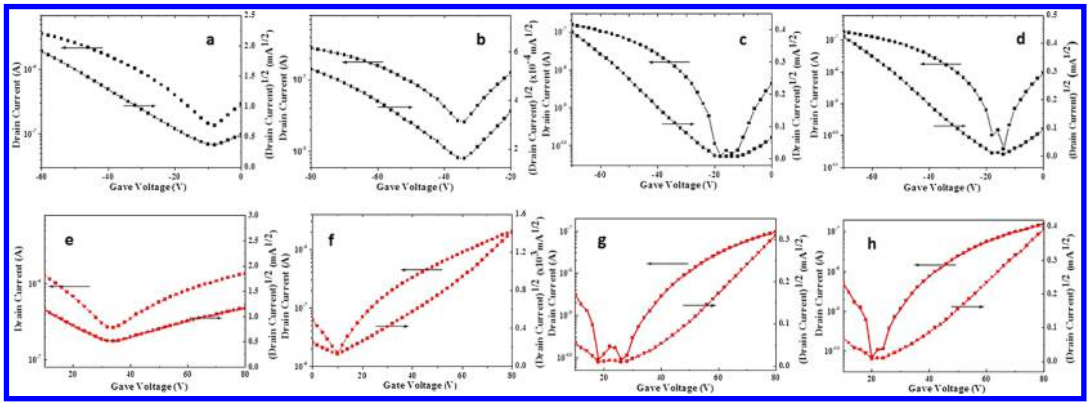

Figure 4. Transfer characteristics of EH−FBT (a and e), EH−DFBT (b and f), DMO−FBT (c and g), and DMO−DFBT (d and h). (spin-cast from chlorobenzene solutions).

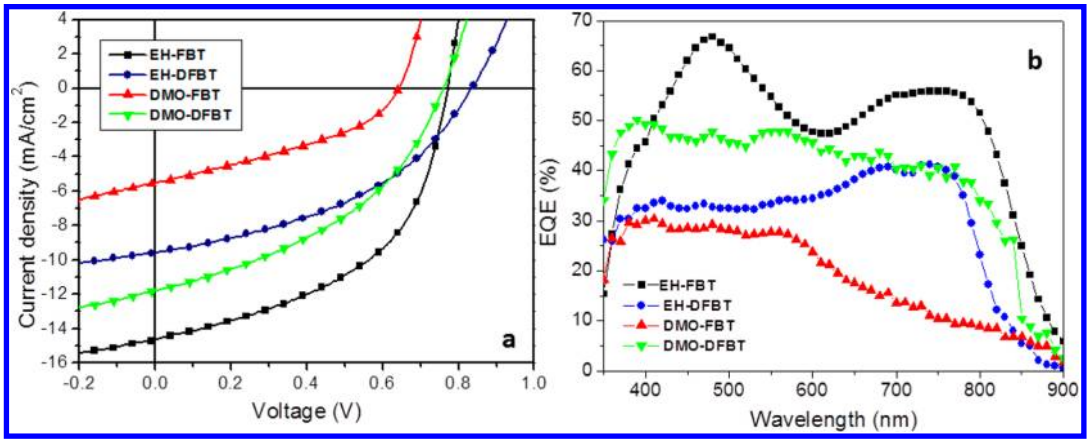

Figure 5. J−V (a) and EQE (b) curves of EH−FBT, EH−DFBT, DMO−FBT, and DMO−DFBT devices.

how the size of alkyl chain and fluoro-substitution influence the charge transport of these polymers, the mobility of these polymers was measured in a bottom-gate, top-contact field-effect transistors (FET) device configuration built on an n-doped silicon wafer (see the Supporting Information for details). Figure 4 showed the transfer characteristics of the polymers under positive and negative gate voltages. All these polymers exhibited clear ambipolar behavior, which is beneficial for the performance of solar cells. The EH−FBT films exhibited a hole-mobility of ~0.014 $cm^2\ V^{-1}\ s^{-1}$ with an on/off ratio of 10^2. This result was the highest hole-mobility among these four polymers, which can be attributed to the shorter π−π stacking distances. Unexpectedly, DMO−DFBT, with the shortest π−π stacking spacing, showed lower device performance compared with that of EH−FBT. The mobility of DMO−DFBT was only $3.5 \times 10^{-4}\ cm^2\ V^{-1}\ s^{-1}$, which may be due to its low molecular weight and unfavorable polymer chain packing. Both EH−DFBT and DMO−FBT showed lower hole-mobilities of 5.0×10^{-4} and 3.0×10^{-4}, respectively due to their longer π−π stacking distance.

It is interesting to observe significant changes of optical, electrochemical, and morphological properties in these polymers by only changing their structures slightly. Furthermore, this resulted in very significant changes of PCE from 1.29% to 5.48% in their BHJ devices. In order to accurately compare these data and interpret the structure−property relationships, photovoltaic devices were all made under the same condition. All devices possessed the configuration of ITO/PEDOT:PSS/polymer:$PC_{71}BM$/C_{60}-bis surfactant/Ag. The optimized polymer to $PC_{71}BM$ ratio of 1:2 was used in the formulation. The active layers were processed from their pure CB solutions without using any additive, except EH−DFBT, which was processed from o-DCB solution, because of its poor solubility in CB. The current−voltage characteristics of the solar cells are shown in Figure 5 with representative performance parameters listed in Table 3.

As shown in Table 3, large V_{oc} differences could be observed due to differences in polymers' electronic properties. It is known that the V_{oc} of a PSC is proportional to the difference between the HOMO level of polymer and the LUMO level of

dx.doi.org/10.1021/ma4009302 | Macromolecules 2013, 46, 5497−5503

Table 3. Summarized Performances of Devices Containing EH−FBT, EH−DFBT, DMO−FBT, and DMO−DFBT

polymer	V_{oc} (V)	J_{sc} (mA cm^{-2})	FF	PCE (%)
EH−FBT	0.76	14.50	0.50	5.48
EH−DFBT	0.84	9.59	0.42	3.37
DMO-FBT	0.65	4.76	0.41	1.29
DMO−DFBT	0.76	11.80	0.41	3.67

$PC_{71}BM$. By lowering the HOMO level, it results in a higher V_{oc}. When DFBT is used, an increase of ∼0.08−0.09 V is seen in the V_{oc}. Surprisingly, the replacement of the shorter and bulkier side-chains with longer side-chains resulted in a significantly increased HOMO level. As a result, the V_{oc} decreased for almost 0.1 V. It is commonly believed that the electronic properties of a conjugated polymer are determined by the composition of the conjugated backbone, whereas the attached alkyl side-chains are thought to be irrelevant. Recently, Gadisa et al.[32] have reported that longer side-chains on the conjugated polymers tend to lower its HOMO level. Li et al.[33] have also reported that the substitution of longer/branched alkyl chains on CPDT tends to lower the HOMO energy level and increased the device V_{oc}. Similar phenomena has also been observed by Thompson et al. for P3HT-based polymers.[34] This is contradictory to our observation that the HOMO levels in deed increased with the increase of the side-chain length. This may be explained by the enhanced intermolecular interactions due to stronger stacking of the DMO side-chain substituted polymer.

Meanwhile, the large change of J_{sc} and FF could also be observed by replacing the shorter and bulkier side-chains of EH−FBT with the longer DMO−FBT to result in a dramatically decreased J_{sc} (from 14.5 to 4.76 mA/cm^2). After the introduction of DFBT, it improves the J_{sc} back to 11.8 mA/cm^2. The external quantum efficiency (EQE) of polymer/$PC_{71}BM$ devices were measured and shown in Figure 5b. It can be seen that the J_{sc} values calculated from the EQE curves under the standard AM 1.5G conditions match well with those obtained from the $J-V$ measurements. The devices showed broad response over the range 350−900 nm. The EH−FBT showed the highest EQE value (50%) between 400 to 800 nm compared to 30% for EH−DFBT, 10% for DMO−FBT and 40% for DMO−DFBT, which is consistent with the result from measured J_{sc}. Our UV−vis and XRD studies showed DMO−FBT is less crystalline. The long and branched side-chain may not only weaken the intermolecular interactions between polymers but also facilitates more PCBM intercalation into polymers. All these can affect exciton recombination and charge transport to result in lower EQE and J_{sc}. On the contrary, the stronger F−H, F−F interactions in DMO−DFBT resulted in better polymer packing and significantly improved EQE and J_{sc}.

In conclusion, we have investigated systematically how alkyl side-chain and F-substitution affect the photovoltaic properties of cyclopentadithiophene-based conjugated polymers. When shorter EH side-chains are replaced with longer DMO side-chains, it resulted in significantly changed electronic properties and morphology of these polymers. The $\pi-\pi$ stacking distances of these polymers significantly affects the mobility measured in their corresponding OFET devices. The shorter $\pi-\pi$ stacking distance of the polymer thin film resulted in higher mobility and FF in their corresponding solar cells. The tuning of F-substitution and side-chain help optimize $\pi-\pi$ stacking, polymer crystallinity, and solubility, which provides valuable insights for the further development of new generation of low band gap materials.

EXPERIMENTAL SECTION

General Characterization Methods. UV−vis spectra were obtained using a Perkin-Elmer Lambda-9 spectrophotometer. The ^{1}H NMR spectra were collected on a Bruker AV 300 spectrometer operating at 300 MHz in d-chloroform solution with TMS as reference. MS spectra were recorded on Bruker Esquire LC-Ion Trap. Cyclic voltammetry of polymer films were measured against Ag/Ag$^+$ as the reference electrode, ITO as working electrode and Pt mesh electrode in an 0.1 M electrolyte containing tetrabutylammonium hexafluoro-phosphate in acetonitrile with a scan rate of 100 mV/s. The molecular weight was measured by a Waters 1515 gel permeation chromatograph with a refractive index detector at room temperature (THF as the eluent). X-ray diffraction measurements were performed on a Bruker D8 X-ray diffractometer using a Cu-Ka source.

Device Fabrication. ITO-coated glass substrates (15 Ω/sq.) were cleaned with detergent, deionized water, acetone, and isopropyl alcohol. A thin layer (ca. 35 nm) of PEDOT:PSS (Baytron P VP AI 4083, filtered at 0.45 μm) was first spin-coated on the precleaned ITO-coated glass substrates at 5,000 rpm and baked at 140 °C for 10 min under ambient conditions. The substrates were then transferred into an argon-filled glovebox. Subsequently, the polymer: $PC_{71}BM$ active layer (ca. 90 nm) was spin-coated on the PEDOT:PSS layer at 600 rpm from a homogeneously blended solution. The solution was prepared by dissolving the polymer and fullerene at weight ratios of 1:2 in chlorobenzene to a total concentration of 12 mg/mL at 110 °C overnight and filtered through a PTFE filter (0.45 μm). All of the substrates were placed on the hot plate at 110 °C for 10 min. After annealing, substrates were briefly transferred out of the glovebox (total ambient exposure <10 min) and a 10 nm thick film of C60-bis surfactant (1 mg/mL in methanol) was spin-coated at 5K rpm.,[35,36] The substrates were then transferred back into the glovebox and annealed at 110 °C for 5 min to drive off any remaining solvent prior to metal deposition. At the final stage, the substrates were pumped down to high vacuum (<2 × 10^{-6} Torr), and silver (100 nm) was thermally evaporated onto the active layer. Shadow masks were used to define the active area (10.08 × 10^{-2} cm^2) of the devices.

Device Characterization. The unencapsulated solar cells were tested under ambient conditions using a Keithley 2400 SMU and an Oriel xenon lamp (450 W) with an AM1.5 filter. The light intensity was calibrated to 100 mW/cm^2 using a calibrated silicon solar cell with a KG5 filter, which has been previously standardized as the National Renewable Energy Laboratory. The current−voltage ($I-V$) characteristics of unencapsulated photovoltaic devices were measured under ambient conditions using a Keithley 2400 source-measurement unit. An Oriel xenon lamp (450 W) with an AM1.5 G filter was used as the solar simulator. The light intensity was set to 1 sun (100 mW cm^{-2}) using a calibrated Hamamatsu silicon diode with a KG5 color filter, which can be traced to the National Renewable Energy Laboratory (NREL). The EQE system usesa lock-in amplifier (Stanford Research Systems SR830) to record the short-circuit current under chopped monochromatic light.

Materials Synthesis. All reagents were purchased from commercial sources without further purification. The synthetic route of monofluoro- (FBT) and difluoro-BT (DFBT) involves a multistep synthesis, starting from 2,5-dibromo-3-fluorobenzene and 2,5-dibromo-3,4-difluorobenzene as shown in our previous work.[23] The synthetic route of monomers **8a** and **8b** is shown in Scheme S1, Supporting Information.

Compound ***8***. To a solution of compound **7** in THF was added *n*-BuLi at −78 °C. The resulting mixture was kept at −78 °C for 30 min then at room temperature for 1h. After cooling to −78 °C, the trimethyltin chloride was added in one portion. The mixture was poured into water after stirring at room temperature overnight and extracted with hexane. The organic phase was dried over anhydrous Na_2SO_4. After removing the solvent under vacuum, a yellow liquid was achieved and used in the next step without further purification.

dx.doi.org/10.1021/ma4009302 | Macromolecules 2013, 46, 5497−5503

8a: ^{1}H NMR (300 MHz, $CDCl_3$, d) 6.96 (t, J = 2.4 Hz, 2H), 1.86 (m, 4H), 1.02−0.93 (m, 18H), 0.76 (t, J = 6.5 Hz, 6H), 0.60 (t, J = 7.3 Hz, 6H), 0.37 (t, 18H). MS (m/z): $[M + H]^+$ calcd for $C_{31}H_{54}S_2Sn_2$, 730.2; found, 730.2.

8b: ^{1}H NMR (300 MHz, $CDCl_3$, d) 6.94 (s, 2H), 1.84 (m, 4H), 1.50(m, 2H), 1.32−1.02 (m, 18H), 084 (d, J = 6.5 Hz, 12H), 0.76 (d, J = 6.5 Hz, 6H), 0.37 (t, 18H). MS (m/z): $[M + H]^+$ calcd for $C_{35}H_{62}S_2Sn_2$, 784.2; found, 784.2.

General Method of Microwave-Assisted Stille Coupling Polymerization. In a 10 mL microwave tube was charged with cyclopentadithiophene monomer (0.5 mmol) and the monofluoro or difluoro-BT(0.48 mmol) in a mixture of *o*-xylenes (2 mL) and DMF (0.2 mL). After being purged with argon for 15 min. $Pd_2(dba)_3$ (0.024 mmol) and P(o-tol)$_3$ (0.087 mmol) were added consequently. Then, the resulted mixture was heated in a microwave reactor at 120 °C for 5 min, 150 °C for 5 min, and 170 °C for 40 min. After cooling to room temperature, the resulted mixture was precipitated by adding into methanol (50 mL) and filtered. The collected precipitate was subjected to Soxhlet extraction with methanol, hexanes, and chloroform. The high molecular weight part was collected and dried under vacuum. The yield and results of the polymers are as follows:

EH−FBT. ^{1}H NMR (*o*-DCB (*o*-$C_6D_4Cl_2$), ppm): 8.55−8.35 (d, br, 2H), 7.66 (br, 1H), 2.23 (br, 2H), 1.40−1.18 (d, br, 32H). Molecular weight: M_n = 25.3 kDa; PDI = 1.58. Yield: 40%.

DMO−FBT. ^{1}H NMR ($CDCl_3$, ppm): 8.15 (br, 2H), 7.70 (br, 1H), 2.03 (br, 4H), 1.44 (br, 2H), 1.42−0.78 (br, 36H). Molecular weight: M_n = 24.6 kDa; PDI = 1.47. Yield 56%.

EH−DFBT. ^{1}H NMR (*o*-DCB (*o*-$C_6D_4Cl_2$), ppm): 8.60−8.45 (d, br, 2H), 2.30 (br, 2H), 1.42−1.15 (d, br, 32H). Molecular weight: M_n = 13.6 kDa; PDI = 1.56. Yield: 20%.

DMO−DFBT. ^{1}H NMR ($CDCl_3$, ppm): 8.23 (br, 2H), 2.08 (br, 4H), 1.52−0.78 (d, br, 38H). Molecular weight: M_n = 11.2 kDa; PDI = 1.15. Yield: 36%.

■ ASSOCIATED CONTENT

Ⓢ Supporting Information

Synthesis of polymers, detailed device fabrications, and characterizations, including AFM images. This material is available free of charge via the Internet at http://pubs.acs.org.

■ AUTHOR INFORMATION

Corresponding Author

*E-mail: (A.K.-Y.J.) ajen@u.washington.edu; (Y.C.) chentangyu@yahoo.com.

Notes

The authors declare no competing financial interest.

■ ACKNOWLEDGMENTS

The authors thank the support from the National Science Foundation (DMR-0120967), the Department of Energy (DE-FC3608GO18024/A000), the Air Force Office of Scientific Research (FA9550-09-1-0426), the Asian Office of Aerospace R&D (FA2386-11-1-4072), and Office of Naval Research (N00014-11-1-0300). A.K.-Y.J. thanks the Boeing Foundation for support. Y.L. expresses thanks for the State-Sponsored Scholarship for Graduate Students from the China Scholarship Council.

■ REFERENCES

(1) He, Z.; Zhong, C.; Su, S.; Xu, M.; Wu, H.; Cao, Y. *Nat. Photon.* **2012**, *6* (9), 591−595.

(2) Cheng, Y.-J.; Yang, S.-H.; Hsu, C.-S. *Chem. Rev.* **2009**, *109* (11), 5868−5923.

(3) Duan, C.; Huang, F.; Cao, Y. *J. Mater. Chem.* **2012**, *22* (21), 10416−10434.

(4) Li, C.-Z.; Yip, H.-L.; Jen, A. K. Y. *J. Mater. Chem.* **2012**, *22* (10), 4161−4177.

(5) Zhou, H.; Yang, L.; You, W. *Macromolecules* **2012**, *45* (2), 607−632.

(6) He, F.; Yu, L. *J. Phys. Chem. Lett.* **2011**, *2* (24), 3102−3113.

(7) Gevaerts, V. S.; Furlan, A.; Wienk, M. M.; Turbiez, M.; Janssen, R. A. J. *Adv. Mater.* **2012**, *24* (16), 2130−2134.

(8) Li, W.; Roelofs, W. S. C.; Wienk, M. M.; Janssen, R. A. J. *J. Am. Chem. Soc.* **2012**, *134* (33), 13787−13795.

(9) Bronstein, H.; Chen, Z.; Ashraf, R. S.; Zhang, W.; Du, J.; Durrant, J. R.; Shakya Tuladhar, P.; Song, K.; Watkins, S. E.; Geerts, Y.; Wienk, M. M.; Janssen, R. A. J.; Anthopoulos, T.; Sirringhaus, H.; Heeney, M.; McCulloch, I. *J. Am. Chem. Soc.* **2011**, *133* (10), 3272−3275.

(10) Liu, F.; Gu, Y.; Wang, C.; Zhao, W.; Chen, D.; Briseno, A. L.; Russell, T. P. *Adv. Mater.* **2012**, *24* (29), 3947−3951.

(11) Ong, K.-H.; Lim, S.-L.; Tan, H.-S.; Wong, H.-K.; Li, J.; Ma, Z.; Moh, L. C. H.; Lim, S.-H.; de Mello, J. C.; Chen, Z.-K. *Adv. Mater.* **2011**, *23* (11), 1409−1413.

(12) Schroeder, B. C.; Ashraf, R. S.; Thomas, S.; White, A. J. P.; Biniek, L.; Nielsen, C. B.; Zhang, W.; Huang, Z.; Tuladhar, P. S.; Watkins, S. E.; Anthopoulos, T. D.; Durrant, J. R.; McCulloch, I. *Chem. Commun.* **2012**, *48* (62), 7699−7701.

(13) Shahid, M.; Ashraf, R. S.; Huang, Z.; Kronemeijer, A. J.; McCarthy-Ward, T.; McCulloch, I.; Durrant, J. R.; Sirringhaus, H.; Heeney, M. *J. Mater. Chem.* **2012**, *22* (25), 12817−12823.

(14) Peng, Q.; Huang, Q.; Hou, X.; Chang, P.; Xu, J.; Deng, S. *Chem. Commun.* **2012**, *48* (93), 11452−11454.

(15) Osaka, I.; Shimawaki, M.; Mori, H.; Doi, I.; Miyazaki, E.; Koganezawa, T.; Takimiya, K. *J. Am. Chem. Soc.* **2012**, *134* (7), 3498−3507.

(16) Wu, J.-S.; Lin, C.-T.; Wang, C.-L.; Cheng, Y.-J.; Hsu, C.-S. *Chem. Mater.* **2012**, *24* (12), 2391−2399.

(17) Hou, J.; Chen, H.-Y.; Zhang, S.; Li, G.; Yang, Y. *J. Am. Chem. Soc.* **2008**, *130* (48), 16144−16145.

(18) Wang, M.; Hu, X.; Liu, P.; Li, W.; Gong, X.; Huang, F.; Cao, Y. *J. Am. Chem. Soc.* **2011**, *133* (25), 9638−9641.

(19) Zhang, Y.; Zou, J.; Cheuh, C.-C.; Yip, H.-L.; Jen, A. K. Y. *Macromolecules* **2012**, *45* (13), 5427−5435.

(20) Albrecht, S.; Janietz, S.; Schindler, W.; Frisch, J.; Kurpiers, J.; Kniepert, J.; Inal, S.; Pingel, P.; Fostiropoulos, K.; Koch, N.; Neher, D. *J. Am. Chem. Soc.* **2012**, *134* (36), 14932−14944.

(21) Price, S. C.; Stuart, A. C.; Yang, L.; Zhou, H.; You, W. *J. Am. Chem. Soc.* **2011**, *133* (12), 4625−4631.

(22) Tsao, H. N.; Cho, D. M.; Park, I.; Hansen, M. R.; Mavrinskiy, A.; Yoon, D. Y.; Graf, R.; Pisula, W.; Spiess, H. W.; Müllen, K. *J. Am. Chem. Soc.* **2011**, *133* (8), 2605−2612.

(23) Zhou, H.; Yang, L.; Stuart, A. C.; Price, S. C.; Liu, S.; You, W. *Angew. Chem., Int. Ed.* **2011**, *50* (13), 2995−2998.

(24) Zhang, Y.; Chien, S.-C.; Chen, K.-S.; Yip, H.-L.; Sun, Y.; Davies, J. A.; Chen, F.-C.; Jen, A. K. Y. *Chem. Commun.* **2011**, *47* (39), 11026−11028.

(25) Son, H. J.; Wang, W.; Xu, T.; Liang, Y.; Wu, Y.; Li, G.; Yu, L. *J. Am. Chem. Soc.* **2011**, *133* (6), 1885−1894.

(26) Xu, Y.-X.; Chueh, C.-C.; Yip, H.-L.; Ding, F.-Z.; Li, Y.-X.; Li, C.-Z.; Li, X.; Chen, W.-C.; Jen, A. K. Y. *Adv. Mater.* **2012**, *24* (47), 6356−6361.

(27) Lei, T.; Dou, J.-H.; Pei, J. *Adv. Mater.* **2012**, *24* (48), 6457−6461.

(28) Yang, L.; Tumbleston, J. R.; Zhou, H.; Ade, H.; You, W. *Energ. Environ. Sci.* **2013**, *6* (1), 316−326.

(29) Coffin, R. C.; Peet, J.; Rogers, J.; Bazan, G. C. *Nat. Chem.* **2009**, *1* (8), 657−661.

(30) Li, Y.; Pan, Z.; Fu, Y.; Chen, Y.; Xie, Z.; Zhang, B. *J. Polym. Sci., Part A: Polym. Chem.* **2012**, *50* (9), 1663−1671.

(31) Zotti, G.; Schiavon, G.; Berlin, A.; Fontana, G.; Pagani, G. *Macromolecules* **1994**, *27* (7), 1938−1942.

(32) Gadisa, A.; Oosterbaan, W. D.; Vandewal, K.; Bolsée, J.-C.; Bertho, S.; D'Haen, J.; Lutsen, L.; Vanderzande, D.; Manca, J. V. *Adv. Funct. Mater.* **2009**, *19* (20), 3300−3306.

(33) Li, Z.; Tsang, S.-W.; Du, X.; Scoles, L.; Robertson, G.; Zhang, Y.; Toll, F.; Tao, Y.; Lu, J.; Ding, J. *Adv. Funct. Mater.* **2011**, *21* (17), 3331−3336.
(34) Burkhart, B.; Khlyabich, P. P.; Thompson, B. C. *Macromolecules* **2012**, *45* (9), 3740−3748.
(35) Li, C.-Z.; Chueh, C.-C.; Yip, H.-L.; O'Malley, K. M.; Chen, W.-C.; Jen, A. K. Y. *J. Mater. Chem.* **2012**, *22* (17), 8574−8578.
(36) O'Malley, K. M.; Li, C.-Z.; Yip, H.-L.; Jen, A. K. Y. *Adv. Energy Mater.* **2012**, *2* (1), 82−86.